

Temperature-dependence of the phase-coherence length in InN nanowires

Ch. Blömers,¹ Th. Schäpers,^{2,*} T. Richter,¹ R. Calarco,¹ H. Lüth,¹ and M. Marso¹

¹*Institute for Bio- and Nanosystems (IBN-1) and JARA Jülich Aachen Research Alliance, Research Centre Jülich GmbH, 52425 Jülich, Germany*

²*Institute for Bio- and Nanosystems (IBN-1), JARA Jülich Aachen Research Alliance, and Virtual Institute of Spinelectronics (VISel), Research Centre Jülich GmbH, 52425 Jülich, Germany*

(Dated: November 1, 2018)

We report on low-temperature magnetotransport measurements on InN nanowires, grown by plasma-assisted molecular beam epitaxy. The characteristic fluctuation pattern observed in the conductance was employed to obtain information on phase-coherent transport. By analyzing the root-mean-square and the correlation field of the conductance fluctuations at various temperatures the phase-coherence length was determined.

Semiconductor nanowires are versatile building blocks for the design of future electronic devices [1, 2, 3, 4]. This includes, e.g. nano-scaled transistors [5, 6], resonant tunneling devices [7], or quantum dot based devices [8, 9], to name just a few. Among the many possible materials suitable for semiconductor nanowires, InN is particularly interesting because of its low energy band gap and its high surface conductivity [10, 11, 12, 13].

At low temperatures electron interference effects often play a prominent role in the transport characteristics of nanostructures. Typical phenomena observed in this regime are weak localization, the Aharonov–Bohm effect, or universal conductance fluctuations [14, 15]. The characteristic length connected to these effects is the phase-coherence length l_ϕ , i.e. the length over which phase-coherent transport is maintained. The length l_ϕ is an important parameter for the design of device structures based on electron interference.

The analysis of conductance fluctuations is one of the possible methods, in order to obtain information on l_ϕ in semiconductor nanostructures [16, 17, 18, 19, 20, 21, 22]. Due to the small dimensions of semiconductor nanowires, often only a limited number of scattering centers are involved in the transport. In this case, pronounced fluctuations in the conductance can be expected, e.g. when the magnet field is varied. This was indeed observed by Hansen *et al.*[23] for InAs nanowires.

In this letter we will exploit the characteristic fluctuation pattern in the magnetoresistance of InN nanowires, in order to obtain information on the phase-coherent transport. By analyzing the root-mean-square and the correlation field of the fluctuation pattern, the temperature dependence of l_ϕ will be determined.

Two InN nanowires of different thickness, prepared by plasma-assisted MBE, were investigated in this study [?]. The wires were grown on a Si (111) substrate at a temperature of 475°C under N-rich conditions. For the growth of the first sample (wire A) a beam equivalent pressure for In of 3.0×10^{-8} mbar was chosen, while for the second sample (wire B) 7.0×10^{-8} mbar was adjusted. As illustrated in Fig. 1 a), using this scheme growth of InN nanowires with a length of approximately 1 μm was

achieved. From photoluminescence measurements a typical overall electron concentration of $5 \times 10^{18} \text{ cm}^{-3}$ was estimated [12].

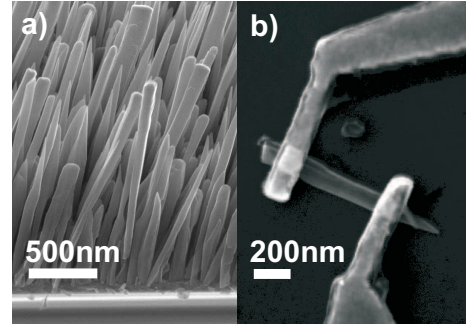


FIG. 1: Scanning electron micrograph of: (a) the as-grown InN nanowires used to prepare sample B, (b) of wire B with the individually defined Ti/Au contact pads.

For the transport measurements of the InN wires, contact pads and adjustment markers were defined on a SiO₂-covered Si (110) wafer. The InN nanowires were dispersed on the patterned substrate, by separating them first from their host substrate in an acetone solution. Subsequently, a droplet of acetone containing the detached InN nanowires was put on the patterned substrate wafer. In the final step, the wires were contacted individually using Ti/Au electrodes defined by electron beam lithography. Wire A had a diameter of $d = 67$ nm with contact pads separated by $L = 410$ nm, while wire B had a diameter of 130 nm with contacts separated by 530 nm. An scanning electron micrograph of wire B is shown in Fig. 1.

The measurements were performed in a He-3 cryostat at temperatures between 0.6 and 25 K. The cryostat was equipped with a 10 T magnet. The magnetic field was oriented perpendicular to the axis of the wires. The magnetoresistance was measured by using a lock-in technique with an ac bias current of 30 nA.

The fluctuation pattern in the total magnetoresistance of wire A at various temperatures is shown in Fig. 2 a). The measurements were performed in a magnetic field

range from -1.5 T to 10.0 T. It can be seen clearly that the fluctuation amplitude decreases substantially if the temperature is increased. Furthermore, one finds that although the amplitude is damped with increasing temperature, the pattern itself is reproduced. As can be seen in Fig. 2 a), due to the two-terminal measurement, the fluctuation pattern is symmetric with respect to the magnetic field B .

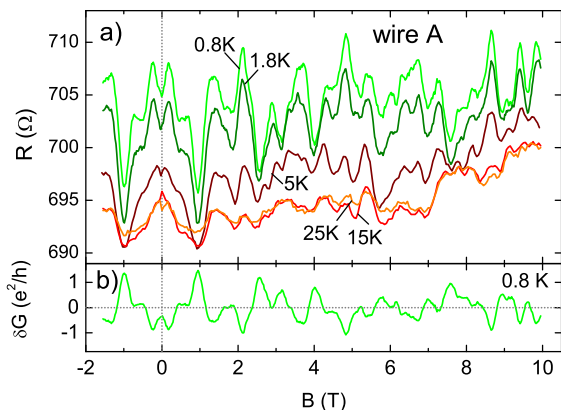


FIG. 2: (a) Magnetoresistance of wire A at temperatures between 0.8 K and 25 K. The measurements show the total two-terminal resistance including the contact resistance. (b) Normalized conductance fluctuations of wire A at 0.8 K.

In order to analyze the electron interference phenomena in detail, first, the fluctuations in the magnetoresistance were converted to the corresponding conductance fluctuations δG . In Fig. 2 b) the fluctuation pattern of the normalized magnetoconductance δG of wire A at 0.8 K is shown. Since the measurements were performed in a two-terminal configuration, first, the contact resistance R_c was subtracted. The contact resistance was estimated by measuring a number of InN wires of the same growth run with comparable diameter but different contact separations. For wire A and B contact resistances R_c of $(330 \pm 50) \Omega$ and $(250 \pm 50) \Omega$, were determined, respectively. After subtracting the contact resistance, the conductance fluctuations $\delta G = G - G_0$ were extracted by subtracting the slowly varying parabolic background contribution G_0 from the total wire conductance. As can be seen in Fig. 2 b), at 0.8 K the conductance fluctuation amplitude is in the order of e^2/h .

We will now focus on the analysis of the temperature-dependence of the conductance fluctuations. The magnitude of δG can be quantified by the root-mean-square of the conductance fluctuations $\text{rms}(G)$, which is defined by $\sqrt{\langle \delta G^2 \rangle}$. Here, $\langle \dots \rangle$ represents the average over the magnetic field. In Fig. 3 a) the $\text{rms}(G)$ of wire A is plotted as a function of temperature. Two regimes are revealed: At temperatures below about 1.5 K, $\text{rms}(G)$ tends to sat-

urate, whereas at temperature above 1.5 K a decrease of $\text{rms}(G)$ proportional $T^{-0.4}$ is observed. A similar decrease proportional to $T^{-0.4}$ was found for wire B above ≈ 2 K, while below 2 K a slightly steeper decrease was observed compared to wire A.

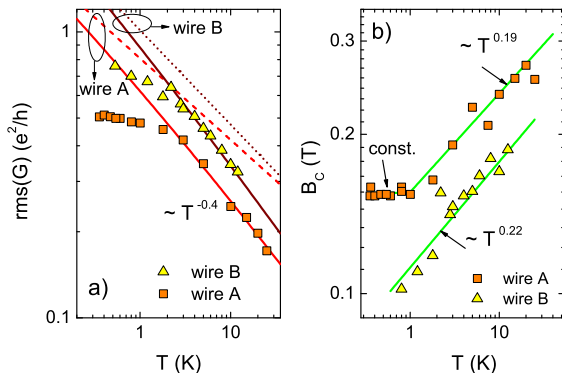


FIG. 3: (a) root-mean-square (rms) of the conductance fluctuations of wire A (\square) and B (\triangle) as a function of temperature. The full and dashed lines show the theoretically expected traces of $\text{rms}(G)$ including and excluding thermal averaging, respectively. (b) Correlation field B_c vs. temperature for wire A and B. The full lines represent the exponential increase of B_c .

Before we proceed to discuss the temperature dependence of $\text{rms}(G)$, we will turn to another important quantity, the correlation field B_c . The correlation field is derived from the autocorrelation function of the conductance fluctuation which is defined as $F(\Delta B) = \langle \delta G(B + \Delta B) \delta G(B) \rangle$. [20] The full width at half maximum of the autocorrelation function $F(B_c) = \frac{1}{2} F(0)$ defines the correlation field B_c . In Fig. 3 b) the temperature dependence of B_c is plotted for both wires. For wire A the correlation field remains constant for temperatures smaller than 1 K, while for larger temperatures B_c increases proportional to $T^{0.19}$. In contrast, for wire B the correlation field B_c monotonically increases with $T^{0.22}$ in the whole temperature range.

In order to estimate the temperature dependence of l_ϕ , we focus the analysis of B_c . No attempt was made to determine l_ϕ directly from $\text{rms}(G)$, because $\text{rms}(G)$ depends on the interplay between two parameters: l_ϕ and l_T [20]. The thermal diffusion length $l_T = \sqrt{\hbar \mathcal{D} / k_B T}$, with \mathcal{D} the diffusion constant, is a measure for the thermal broadening. In contrast, B_c does not depend on thermal broadening effects, i.e. on l_T [22]. Since in our wires the diameter d exceeds the elastic mean free path l_e , l_ϕ was determined from B_c using the expression for the diffusive regime: $l_\phi \approx \Phi_0 / B_c d$, with $\Phi_0 = h/e$ the magnetic flux quantum [20, 22]. The results for sample A are shown in Fig. 4 a). For $T < 1.5$ K the calcu-

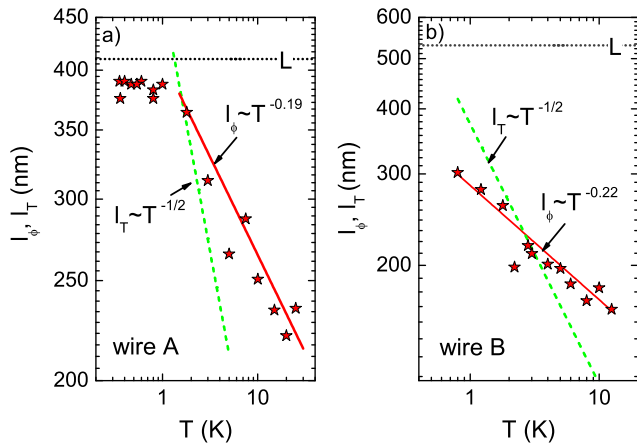


FIG. 4: (a) Phase-coherence length l_ϕ of wire A determined from B_c as a function of temperature (\star). The solid line represents the $T^{-0.19}$ -dependence of l_ϕ above 1.5 K. The dashed line corresponds to the expected temperature dependence of l_T . The wire length L is indicated by the dotted line. (b) Corresponding values for wire B.

lated values of l_ϕ saturate at about the wire length L , indicating that phase coherence is maintained over the complete length. Above 1.5 K, l_ϕ decreases with increasing temperature following a dependence proportional to $T^{-0.19}$. Using the same procedure as described above, l_ϕ was determined from B_c for wire B, as well. As can be seen in Fig 4 b), l_ϕ monotonously decreases with temperature following a dependence proportional to $T^{-0.22}$ in the whole temperature range. Consequently, one can state that for this wire l_ϕ is always smaller than L in the temperature range considered here. For both wires the temperature dependence of l_ϕ is slightly smaller than the theoretically expected dependence proportional to $T^{-1/3}$ [24].

Using the interpolation formula derived by Beenakker and van Houten [22]:

$$\text{rms}(G) = \alpha \frac{e^2}{h} \left(\frac{l_\phi}{L} \right)^{3/2} \left[1 + \frac{9}{2\pi} \left(\frac{l_\phi}{l_T} \right) \right]^{-1/2}, \quad (1)$$

the temperature dependence of $\text{rms}(G)$ was estimated. The formula is valid for $l_\phi \approx l_T < L$. Ideally, the constant α has a value of $\sqrt{6}$. The calculated values for wire A and B using Eq. (1) are shown in Fig. 3. One, finds that at $T > 1$ K the experimental values of $\text{rms}(G)$ vs. T fit very well to the theoretical curves. The values of α with 0.38 and 1.32 for wire A and B, respectively, deviate to some extent from the theoretically expected value. This can be attributed to uncertainties in the determination of R_c affecting the amplitude of $\text{rms}(G)$. For comparison, the $\text{rms}(G) \propto (l_\phi/L)^{3/2}$ curves, representing the case of neglected thermal averaging, are also shown in Fig. 3. One finds that in this case the decrease of $\text{rms}(G)$ is too

small. The fact that thermal smearing has to be considered is also supported by comparing l_T to l_ϕ (cf. Fig. 4). Here, one finds that l_ϕ and l_T are in the same order of magnitude. At lower temperatures ($T < 1$ K) the smaller slope of $\text{rms}(G)$ can be explained by the reduced effect on l_T and to the fact that l_ϕ exceeds or approaches L .

In summary, the phase coherence length l_ϕ of InN nanowires was determined by analyzing the characteristic conductance fluctuation pattern. For the shorter wire it is found that at low temperatures l_ϕ exceeds the wire length L , while at temperatures above 1.5 K $l_\phi < L$ and continuously decreases with increasing T . In contrast for the longer wire (sample B) l_ϕ was smaller than L in the complete temperature range. Our investigations demonstrate, for short InN nanowires phase coherent transport can be maintained along the complete length.

* Electronic address: th.schaepers@fz-juelich.de

- [1] L. Samuelson, C. Thelander, M. T. Björk, M. Borgström, K. Deppert, K. A. Dick, A. E. Hansen, T. Martensson, N. Panev, A. I. Persson, et al., *Physica E* **25**, 313 (2004).
- [2] W. Lu and C. M. Lieber, *J. Phys. D: Appl. Phys.* **39**, R387 (2006).
- [3] C. Thelander, P. Agarwal, S. Brongersma, J. Eymery, L. Feiner, A. Forchel, M. Scheffler, W. Riess, B. Ohlsson, U. Gösele, et al., *Materials Today* **9**, 28 (2006).
- [4] K. Ikejiri, J. Noborisaka, S. Hara, J. Motohisa, and T. Fukui, *J. Cryst. Growth* **298**, 616 (2007).
- [5] T. Bryllert, L.-E. Wernersson, T. Lowgren, and L. Samuelson, *Nanotechnology* **17**, 227 (2006).
- [6] Y. Li, J. Xiang, F. Qian, S. Gradecak, Y. Wu, H. Yan, D. Blom, and C. M. Lieber, *Nano Letters* **6** (2006).
- [7] M. T. Björk, B. J. Ohlsson, C. Thelander, A. I. Persson, K. Deppert, L. R. Wallenberg, and L. Samuelson, *Appl. Phys. Lett.* **81**, 4458 (2002).
- [8] S. D. Franceschi, J. A. van Dam, E. P. A. M. Bakkers, L. Feiner, L. Gurevich, and L. P. Kouwenhoven, *Appl. Phys. Lett.* **83**, 344 (2003).
- [9] C. Fasth, A. Fuhrer, M. T. Bjork, and L. Samuelson, *Nanoletters* **5**, 1487 (2005).
- [10] C. H. Liang, L. C. Chen, J. S. Hwang, K. H. Chen, Y. T. Hung, and Y. F. Chen, *Appl. Phys. Lett.* **81**, 22 (2002).
- [11] C.-Y. Chang, G.-C. Chi, W.-M. Wang, L.-C. Chen, K.-H. Chen, F. Ren, and S. J. Pearton, *Appl. Phys. Lett.* **87**, 093112 (2005).
- [12] T. Stoica, R. J. Meijers, R. Calarco, T. Richter, E. Sutter, and H. Lüth, *Nano Letters* **6**, 1541 (2006).
- [13] R. Calarco and M. Marso, *Applied Phys. A* **87**, 499 (2007).
- [14] C. W. J. Beenakker and H. van Houten, in *Solid State Physics*, edited by H. Ehrenreich and D. Turnbull (Academic, New York, 1991), vol. 44, p. 1.
- [15] J. J. Lin and J. P. Bird, *J. Phys.: Cond. Mat.* **14**, R501 (2002).
- [16] C. P. Umbach, S. Washburn, R. B. Laibowitz, and R. A. Webb, *Phys. Rev. B* **30**, 4048 (1984).
- [17] A. D. Stone, *Phys. Rev. Lett.* **54**, 2692 (1985).
- [18] P. A. Lee and A. D. Stone, *Phys. Rev. Lett.* **55**, 1622

- (1985).
- [19] B. Al'tshuler, Pis'ma Zh. Eksp. Teo. Fiz. [JETP Lett. **41**, 648-651 (1985)] **41**, 530 (1985).
- [20] P. A. Lee, A. D. Stone, and H. Fukuyama, Phys. Rev. B **35**, 1039 (1987).
- [21] T. J. Thornton, M. Pepper, H. Ahmed, G. J. Davies, and D. Andrews, Phys. Rev. B **36**, 4514 (1987).
- [22] C. W. J. Beenakker and H. van Houten, Phys. Rev. B **37**, 6544 (1988).
- [23] A. E. Hansen, M. T. Börk, C. Fasth, C. Thelander, and L. Samuelson, Phys. Rev. B **71**, 205328 (2005).
- [24] B. L. Al'tshuler, A. G. Aronov, and D. E. Khmel'nitsky, J. Phys. C (Sol. State Phys.) **15**, 7367 (1982).